A New Fault Diagnostic Strategy for Photovoltaic Arrays through Artificial Neural Network

1st Amanda Costa Maia
Laboratory of Energy Processing and Control
Federal University of Pampa
Alegrete, Brazil
amandamaia.aluno@unipampa.edu.br

2nd Guilherme Sebastião da Silva
Laboratory of Energy Processing and Control
Federal University of Pampa
Alegrete, Brazil
guilhermesilva@unipampa.edu.br

***Abstract*—Photovoltaic systems' faults can cause a power reduction, the decrease in the useful life and irreversible damages on the photovoltaic cells. This paper presents a strategy able to diagnosticate the photovoltaic array fault according to the Brazilian regulatory standard NBR 16274. Therefore, the fault diagnostic is based on the PV array I-V curve which is used to calculate the inputs of a multilayer perceptron artificial neural network (ANN). The results shown in this paper demonstrate the ANN with a compact structure and good accuracy. Moreover, it shows the ANN can classify all faults of the NBR 16274 with 99.3% of accuracy.**

***Index Terms*—Artificial Neural Network; Classification; Defects; I-V Curve; Multilayer Perceptron.**

I. Introduction

The photovoltaic (PV) systems has grown on Brazil since the government regulation and incentives accomplished in 2012 [1]. Beyond that, other facts contribute for the growth, such as, the PV system price decrease and the concern about the environment [2].

As the number of PV installations has increased in recent years, the maintenance will increase as well [3]. Thus, there is a equipment necessity to assist the preventive maintenance and commissioning of PV arrays [4].

There are main types of problems that occur in continuous current: constant energy lost (degradation and defects), variable energy lost (shading) and obstruction [5]. Each one of these situations can generate irreversible damage in PV cells and significantly power lost.

The main methods to diagnose in PV array faults according with [5] are: climatic data methods, current analyses method, current and voltage derivative method, maximum power points method and artificial neural network method.

The artificial neural network (ANN) method presents good accuracy, fast processing, and better fault diagnostic accuracy, when ANN is compared with other methods. Despite, the other method afore mentioned are easier to implement, because do not need the ANN training, but they have lower identification and classification capacity then ANN technique [4].

The method implemented in the paper has the objective to diagnosticate PV array faults to assist the preventive maintenance and commissioning of PV array. Its differences and advantages are: the multilayer perceptron ANN has a simple structure, the faults classification are based on the Brazilian regulatory standard NBR 16274 [6], and the inputs on the ANN are an array data based on the I-V curve and the local measurement of the temperature and the irrandiance.

The current per voltage curve (I-V curve) defines and characterizes the photovoltaic modules behavior. Therefore, when the I-V curve its correctly analyzed can be established the arrays conditions [7], and, consequently, faults and defects can be identify by the I-V curve [8].

In this paper, a novel strategy using multilayer perceptron ANN is proposed to diagnose PV array faults through the I-V curve according to the faults described by the Brazilian regulatory standard NBR 16274. For that, it is was developed an algorithm to simulate mathematically the I-V curve, training the ANN and identify possible defects and its causes.

II. Characteristic curve of a photovoltaic array

The PV cell has a non-linear behavior between the current and voltage, and as a consequence, its understanding become complex [9]. According with the literature, a simple and faithful way to represent the current of the PV cells it is through one diode model, represented in (1).

$$I_{pv} = I_{ph} - I_0 \times e^{\left(q \times \frac{V_{pv} + I_{pv} \times R_s}{a \times k \times T}\right)} - \frac{V_{pv} + I_{pv} \times R_s}{R_{sh}} \quad (1)$$

Where, I_{pv}: output current (A); I_{ph}: photo-generated current by the cell (A); I_0: reverse saturation current (A); q: electron charge (1.62×10^{-19} C); a: ideality factor; k: Boltzmann constant ($1.381 \times 10^{-23} m^2 \times kg/s^2 \times K$); T: cell temperature (K); R_{sh}: shunt resistance (Ω); R_s: series resistance (Ω) [10]. Notices that (1) is a transcendental equation, however it is possible to trace the photovoltaic cell's I-V curve, shown on Fig. 1.

The main points of the I-V curve are: the short-circuit current (I_{sc}) that represent the current when the PV terminals are in short-circuit [11], the open circuit voltage (V_{oc}) is the voltage measurement without any charge in the PV terminals, and the most important point in the I-V curve is the maximum power point, composed by the current at maximum power (I_{mpp}) and the voltage at maximum power (V_{mpp}).

On the photovoltaic generation occurs climatic variations, such, irradiance, temperature and shading. Each one of this

Fig. 1. Photovoltaic cell's generic I-V curve.

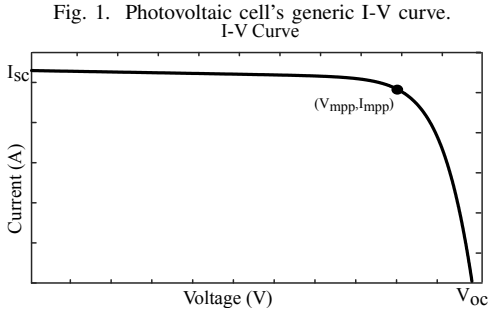

factors decrease the power generate by the PV cell and changes the I-V curve [11].

On a PV cell, as much the irradiance increase, the photo-generate current will increase as well, represented in (2). The V_{oc} grows logarithmically with the irradiance due to dependence between the current and voltage shown on (1).

$$I_{sc} = I_{sc}^{stc} \times \frac{G}{1000} \tag{2}$$

Where, G: irradiance in the PV cell (W/m²); I_{sc}^{stc}: short-circuit current at standard test conditions (A). The Fig. 2 shows the current behavior depending of the irradiance.

The PV cell has a different behavior when the temperature change, as high is the temperature, lower is the voltage and the power, however the current increase [11]. The voltage changes according with (3) and the current with (4).

$$V_{oc} = V_{oc}^{stc} \times (1 - \beta \times \Delta T) \tag{3}$$

$$I_{sc} = I_{sc}^{stc} \times (1 + \alpha \times \Delta T) \tag{4}$$

V_{oc}^{stc}: open circuit voltage at standard test conditions (V); β: V_{oc} temperature coefficient; ΔT: temperature variation (°C); α: I_{sc} temperature coefficient. This feature can be seen on Fig. 2.

Fig. 2. Irradiance and temperature effect on I-V curve.

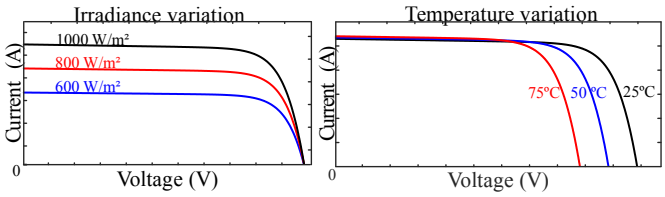

Furthermore, some inner PV cells features can change the I-V curve, such as, series resistance and the shunt resistance. The series resistance represents the lost duo to semiconductor material resistance and the cells' metallic contacts, its value is ideally 0 Ω. Beyond that, the shunt resistance represents the leakage current, material impurities and cells' imperfections, its ideally value is ∞ Ω. The Fig. 3 shows the effects of those resistances in the I-V curve.

Fig. 3. R_s and R_{sh} alteration on the I-V curve.

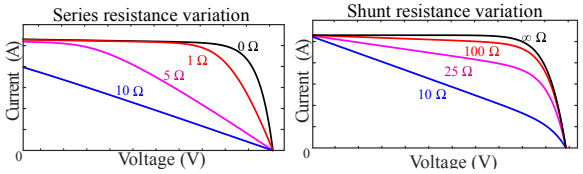

Others situations that change the I-V curve are shade, there are three types of them, such, soft shade, hard shade and partially shaded, and each has a different impact on the I-V curve [12]. The soft shading is caused by the uniformly sediment accumulation in the module surface, and as a consequence there is a reduction in the irradiance that reaches the PV cell [13]. Hard shading is provoked by a total covered cell, when this occurs there is a open circuit voltage reduction [14], as seen in Fig. 4.

Fig. 4. Soft shading and hard shading in the I-V curve.

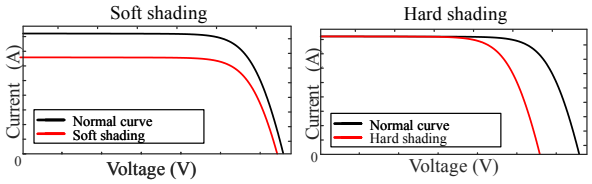

The partially shading distort the I-V curve, creating inflection points (V_{inf}), an example of partially shading can be seen in the Fig. 5.

Fig. 5. Partially shading in the I-V curve.

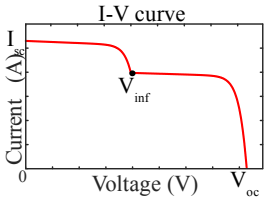

A. *Brazilian regulatory standard NBR 16274*

According with the standard NBR 16274, there are five main faults that can occur in a PV array, also determine their linked with the variation in the I-V curve. The Fig. 6 shows each one of this differences mentioned on NBR 16274.

Fig. 6. Main defects that occurs in a PV array.

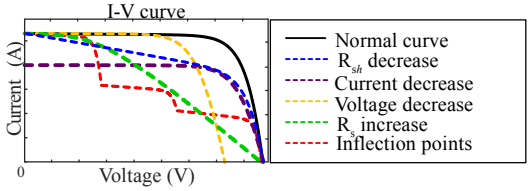

- R_s increase: caused by conductors' damage, modules degradation or cell manufacture's problems [15].
- Voltage decrease: caused by hard shading or short circuit at bypass diode.
- Current decrease: happens when are dust accumulation on module surface, cells degradation or current sensors calibration's problems.
- Inflection points: caused by partially shading, cells damage or improperly bypass diode operation [15].
- R_{sh} decrease: caused by PV cells damage or partially shading.

III. Proposed PV Fault Diagnosis Strategy

The proposed strategy presented in this section uses an multilayer ANN to classify the faults in PV arrays. The ANN and the system are described below.

A. Artificial neural network

Artificial neural networks are systems based on biologic neuron capable of solving problems, such: classification, categorization, approximation, prediction and optimization [16]. The ANN needs training to define the synaptic weights aiming to achieve suitable output for specific input signals [17].

The main classification ANN types are: perceptron, adaline and multilayer perceptron. Duo this research's characteristics will be used a multilayer perceptron because its solve non-linear problems [18]. The multilayer perceptron (MLP) neural network is composed by the input, one or two hidden layers and the output [19]. The Fig. 7 shows a MLP with two hidden layers.

Fig. 7. Multilayer Perceptron Artificial Neural Network.

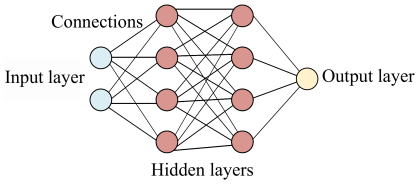

The MLP that has one hidden layer can approach any linearly separable function, on the other hand, a MLP that has two hidden layers can approach any function, such non-linear, separable and transcendental functions.

B. System for faults diagnosis in PV arrays

The proposed system is seen on Fig. 8, and the inputs are: I-V curve, the module irradiance and the PV module data. The information are passed on the ANN and the output are the array conditions according with NBR 16274.

The database is created for the purpose of training the neural network. This database is construct from a mathematics model of the PV cell. Its flowchart is shown on Fig. 9. The database has the same proposed system inputs, and aims to provide the arrays' I-V curve [6]. Firstly, it is calculated the series resistance, shunt resistance e the reverse saturation current

Fig. 8. System for faults diagnosis in PV arrays.

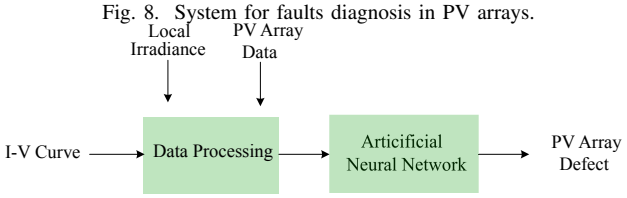

(intrinsic parameters [20]). Then, from the chosen fault and the parameters on Table I is created the I-V curve.

Fig. 9. Algorithm to generate the database.

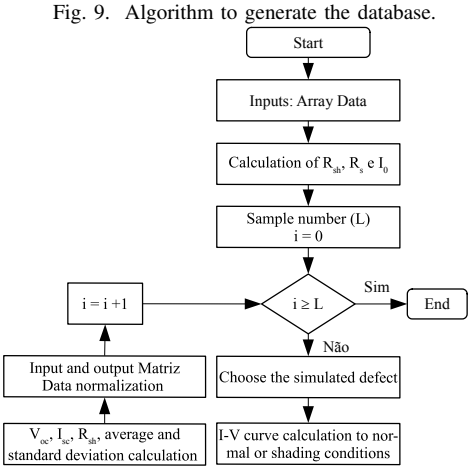

TABLE I
Range of Assigned Values

Description	Assigned range
Irradiance	400 to 1000 W/m²
Temperature	10 to 60 °C
Number of series modules	1 to 10
Number of parallel modules	1 to 10

The database has two outputs in matrix form, the X matrix represented in (5) owns the I-V curve characteristics, and M is the output current average. Furthermore, it is essential that the matrix values are normalized [21].

$$X = \begin{pmatrix} G_1 & V_{oc,1} & I_{sc,1} & R_{sh,1} & M_1 & D_1 \\ \cdot & \cdot & & & & \cdot \\ \cdot & & & \cdot & & \cdot \\ G_m & V_{oc,m} & I_{sc,m} & R_{sh,m} & M_m & D_m \end{pmatrix}^T \quad (5)$$

The matrix Y, shown in (6), represents the arrays conditions according with NBR 16274. In addition, each output matrix represents a defect, presented in Table II.

$$Y = \begin{pmatrix} y_{11} & y_{12} & y_{13} & y_{14} & y_{15} & y_{16} \\ \cdot & \cdot & & & & \cdot \\ \cdot & & & \cdot & & \cdot \\ y_{m1} & y_{m2} & y_{m3} & y_{m4} & y_{m5} & y_{m6} \end{pmatrix}^T \quad (6)$$

TABLE II
DATABASE OUTPUT MATRIX

Defect type	ANN predict output
Normal operation conditions	1 0 0 0 0 0
R_{sh} decrease	0 1 0 0 0 0
Inflection points	0 0 1 0 0 0
I_{sc} decrease	0 0 0 1 0 0
V_{oc} decrease	0 0 0 0 1 0
R_s increase	0 0 0 0 0 1

To create a multilayer perceptron ANN was used the $Matlab$ software [22]. In a supervised learning the output vector is compared with the target vector, generating an error. Given this error the weights are adjusted until the output match with the desired output, the creating process is given by Fig. 10.

Fig. 10. ANN creation and training.

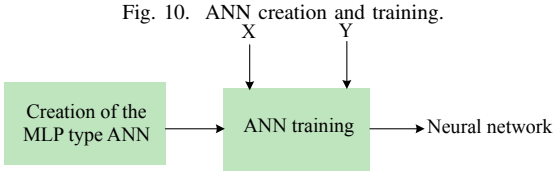

The proposed system to diagnose the faults in a PV arrays can be seen in Fig 11. Its inputs are the I-V curve, PV arrays data, and local irradiance. The algorithm associates the specified defect in NBR 16274 and its probably causes.

Fig. 11. Data treatment flowchart.

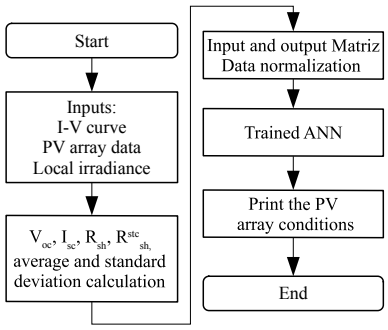

IV. RESULTS

The following results correspond to the ANN learning and the data treatment algorithm.

A. Multilayer perceptron ANN learning

The neural network is given by the database created to emulate the real PV modules functioning conditions. The modules $Kyocera$ KD210GX-LP composes the array used to generate the samples, the module parameters are presented in Table III.

For the database was generated 750 samples with rand values of irradiance, temperature, series and parallel module numbers. The MLP neural network was configured using the

TABLE III
MODULE KD210GX-LP PARAMETERS

Description	Value
Maximum Power	P_{max} = 210W
Maximum Power Voltage	V_{mpp} = 26.6V
Maximum Power Current	I_{mpp} = 7.9A
Open circuit voltage	V_{oc} = 33.2V
Short circuit current	I_{sc} = 8.58A
Cells number	N = 54
Ideality factor	a = 1.3
V_{oc} temperature coefficient	β = -1,2×10^{-1}V/°C
I_{sc} temperature coefficient	α = 5,15×10^{-3}A/°C

TABLE IV
ANN TRAINING CRITERIA

Description	Value
Learning rate	0.01
Momentum	0.9
Stopping criteria	1×10^{-6}
Epoch limits	3000

Table IV criteria. Also, it was used 70 % of the samples for training, 20 % for testing and 10 % for validation.

Moreover, using the $Matlab$ software was created the ANN with the following characteristics: hyperbolic tangent activation function and levenberg-marquardt training algorithm. The number of hidden layers and the number of neurons was defined empirically. However, a several tests were made using the criteria of mean square error (MSE) and the test and training hit ratio. The best results are shown on Table V.

TABLE V
MSE AND TEST AND TRAINING HIT RATIO FOR DIFFERENT TOPOLOGIES

First layer	MSE %	Training hit ratio %	Test hit ratio %
5	5.1×10^{-2}	99.73	98.67
6	2.7×10^{-2}	99.82	98.6
7	2.3×10^{-2}	99.86	98.99
8	1.9×10^{-2}	99.87	98.74
9	2.22×10^{-2}	99.89	98.79
10	4.44×10^{-2}	99.76	98.93

Based on the Table V results, it was chosen the ANN with eight neurons in the hidden layer, the MLP topology is shown on Fig. 12.

Fig. 12. Multilayer perceptron network.

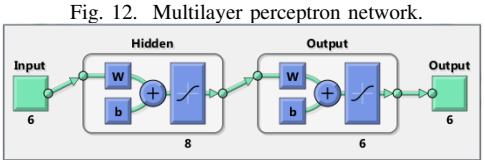

The ANN error performance is seen on Fig. 13, and the error of 0.003845 was reached on epoch 16.

Beyond, on the test step was used 150 samples to generate the confusion matrix, on Fig. 14. This matrix shows the amount of samples that were correctly classified, and also, informs the network accuracy, in this case was 99.3 %.

Fig. 13. ANN error performance during the training. Best Validation Performance is 0.003845 at epoch 16

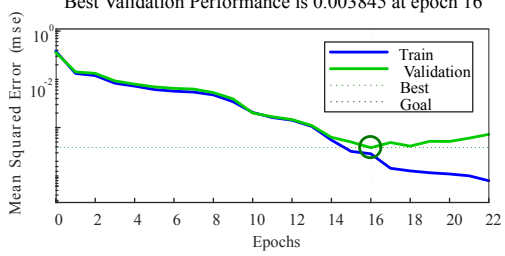

Fig. 14. Confusion matrix.

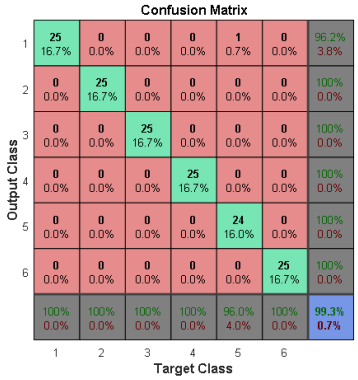

B. Treatment data algorithm

To verify the generalization capacity of the ANN and the functioning of the proposed system it was used a different module to compose the array, and generated another randomly operation conditions. The module used was the $Kyocera$ KC40T and its parameters are represented on Table VI. In the algorithm are tested the conditions specify on the NBR 16274.

TABLE VI
MODULE KC40T PARAMETERS

Description	Value
Maximum Power	P_{max} = 43W
Maximum Power Voltage	V_{mpp} = 17.4V
Maximum Power Current	I_{mpp} = 2.48A
Open circuit voltage	V_{oc} = 21.7V
Short circuit current	I_{sc} = 2.65A
Cells number	N = 36
Ideality factor	a = 1.3
V_{oc} temperature coefficient	β = -8.21×10^{-2}V/°C
I_{sc} temperature coefficient	α = 1.06×10^{-3}A/°C

The standard I-V curve for normal operational conditions, according with Fig. 15, the array is composed with eight modules in series and seven in parallel, and irradiance of 846 W/m². The algorithm detects that active neuron and prints the message: "The array is in normal operational conditions".

On the Fig. 16, to compose the array was used seven modules in series and seven in parallel, and irradiance of 853 W/m², also it can be seen the consequences of the defect. The algorithm detects that the last neuron is active, and prints the

Fig. 15. Results for normal operational conditions.

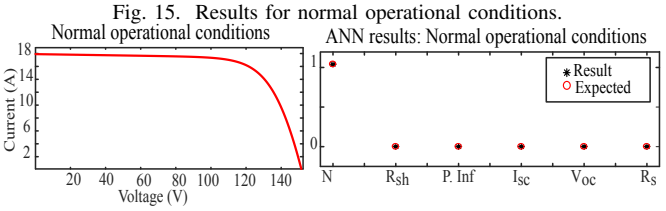

following message: "Damage or wiring failure, PV modules connections failure and it is recommended to check the quality of the system wires".

Fig. 16. Results for R_s increase.

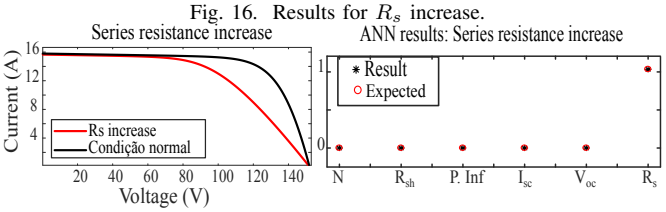

On Fig. 17 the array has 8 modules in series and 8 in parallel, and irradiance of 512 W/m², it is presented the open circuit voltage decrease. The algorithm prints the message: "Number of series modules incorrect, hard shading and bypass diode operating incorrectly".

Fig. 17. Results for V_{oc} decrease.

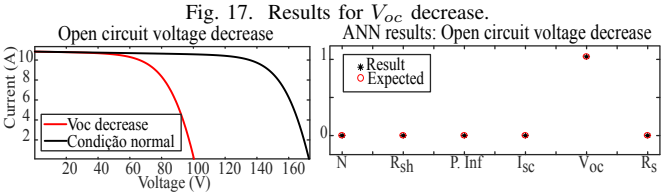

The array on Fig. 18 is composed with nine modules in series and eight in parallel, and irradiance of 420 W/m². The report present for the defect "I_{sc} decrease" is: "The array is dirty or obstructed, the modules are degraded, modules data incorrect or calibration problems in the current meter".

Fig. 18. Results for I_{sc} decrease.

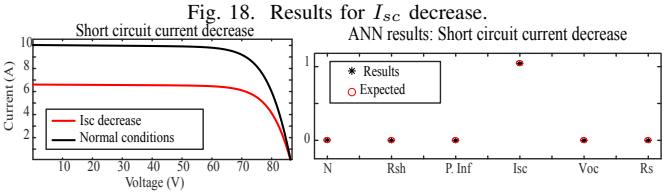

The defect presented on Fig. 19 generates several maximum power points decreasing the power, the system is composed with three modules in series. The possible causes are: partially shading, damage cells and short circuited bypass diode.

The defect shunt resistance decrease is represented in Fig. 20, the PV array is composed with seven series modules and nine in parallel and an irradiance of 422 W/m². The possible cause are: PV cells or interconnections defects, modules short circuit current divergence.

Fig. 19. Results for inflection points.

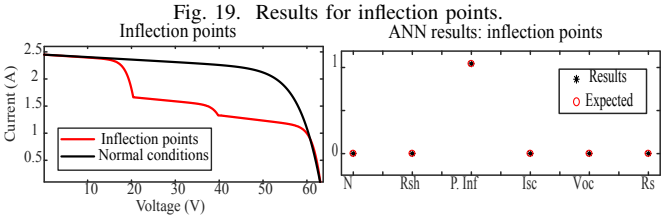

Fig. 20. Results for R_{sh} decrease.

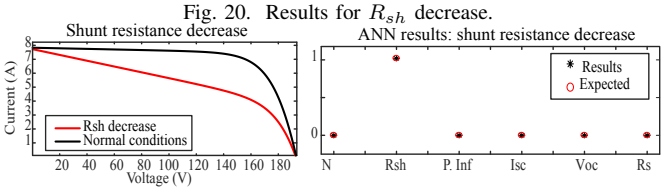

The Table VII compare the proposed system with others methods for defects classification in the literature.

TABLE VII
COMPARISON BETWEEN LITERATURE METHODS.

Parameter	Proposed system	[23]	[24]
System input	I-V curve, irradiance and array data	Thermal images	Aerea images
Defects	R_{sh} decrease, inflection point, I_{sc} decrease, V_{oc} decrease, and R_s increase	Broken edge, dusty, cracks, hotspots and defects in big areas	dust shading, delamination, grid corrosion, snail trails, and degradation
Algorithm	Multilayer perceptron	Convolutional neural network	Convolutional neural network
Accuracy	99.3%	97.2%	98.5%

V. CONCLUSION

The paper presented a system that using a multilayer perceptron ANN able to detect and classify according with the standard NBR 16274. The inputs' system are PV modules parameters available on datasheet, the I-V curve, irradiance.

The results showed that the system was classified correctly the faults: normal operational conditions, R_{sh} increase, inflection points, I_{sc} decrease, V_{oc} decrease and R_s increase, presenting an accuracy of 99.3 %.

The main advantages of the system is not to be necessary technical knowledge of the I-V curve to identify and classify faults. Furthermore, the ANN used to classify has a simple architecture, demanding a lower processing power. The system's disadvantage is a necessity to mathematical modeling of the PV module for the ANN training.

The PV array fault has consequences, such as, generated power reduction, irreversible cells damage and cells burning, the proposed system assists in the PV array maintenance, besides to have a bigger agility to correct the faults.

REFERENCES

[1] I. International Energy Agency, "World Energy Outlook 2018," 2018. www.iea.org/t&c/.

[2] I. International Energy Agency, "Data and statistics," Brazil, 2021. https://www.iea.org/data-and-statistics/data-browser?country=BRAZIL &fuel=Energy supply&indicator=TESbySource.

[3] Karatepe, Engin, and Takashi Hiyama. "Controlling of artificial neural network for fault diagnosis of photovoltaic array." 2011 16th International Conference on Intelligent System Applications to Power Systems. IEEE, 2011.

[4] Jiang, Lian Lian, and Douglas L. Maskell. "Automatic fault detection and diagnosis for photovoltaic systems using combined artificial neural network and analytical based methods." 2015 International Joint Conference on Neural Networks (IJCNN). IEEE, 2015.

[5] Chine, W., et al. "Fault detection method for grid-connected photovoltaic plants." Renewable Energy 66 (2014): 99-110.

[6] Maia, Amanda C., et al. "Method to trace the photovoltaic characteristic curves under partial shading conditions." 2019 IEEE PES Innovative Smart Grid Technologies Conference-Latin America (ISGT Latin America). IEEE, 2019.

[7] Huang, Jun-Ming, Rong-Jong Wai, and Wei Gao. "Newly-designed fault diagnostic method for solar photovoltaic generation system based on IV-curve measurement." IEEE Access 7 (2019): 70919-70932.

[8] M. Young, The Technical Writer's Handbook. Mill Valley, CA: University Science, 1989.

[9] Suykens, Johan AK, and Joos Vandewalle. "Training multilayer perceptron classifiers based on a modified support vector method." IEEE transactions on Neural Networks 10.4 (1999): 907-911.

[10] Cotfas, Daniel Tudor, Petru Adrian Cotfas, and Angel Cataron. "Using the genetic algorithm to determine the parameters of photovoltaic cells and panels." 2018 International Symposium on Electronics and Telecommunications (ISETC). IEEE, 2018.

[11] Ma, Xuan, et al. "Data-Driven I–V Feature Extraction for Photovoltaic Modules." IEEE Journal of Photovoltaics 9.5 (2019): 1405-1412.

[12] Hocaoglu, Fatih Onur, et al. "Comparison of experimentally obtained IV curves of different PV modules." 2018 9th International Renewable Energy Congress (IREC). IEEE, 2018.

[13] Seyedmahmoudian, Mohammadmehdi, et al. "Analytical modeling of partially shaded photovoltaic systems." Energies 6.1 (2013): 128-144.

[14] Pendem, Suneel Raju, and Suresh Mikkili. "Performance evaluation of series, series-parallel and honey-comb PV array configurations under partial shading conditions." 2017 7th International Conference on Power Systems (ICPS). IEEE, 2017.

[15] ASSOCIAÇÃO BRASILEIRA DE NORMAS TÉCNICAS (ABNT). "NBR 16274. Sistemas fotovoltaicos conectados à rede-requisitos mínimos para documentação, ensaios de comissionamento, inspeção e avaliação de desempenho." (2014).

[16] Wilamowski, Bogdan M. "Neural network architectures and learning algorithms." IEEE Industrial Electronics Magazine 3.4 (2009): 56-63.

[17] Rodríguez, Juan David Bastidas, Carlos Andrés Ramos-Paja, and Edinson Franco Mejía. "Modeling and parameter calculation of photovoltaic fields in irregular weather conditions." Ingeniería 17.1 (2012): 37-48.

[18] Lin, Xue, et al. "Designing fault-tolerant photovoltaic systems." IEEE Design & Test 31.3 (2013): 76-84.

[19] Gori, Marco, Franco Scarselli, and Ah Chung Tsoi. "On the closure of the set of functions that can be realized by a given multilayer perceptron." IEEE transactions on neural networks 9.6 (1998): 1086-1098.

[20] Cornelius, Richard G., et al. "Method to trace the photovoltaic characteristic curve with reverse voltage for shading conditions." 2019 IEEE 15th Brazilian Power Electronics Conference and 5th IEEE Southern Power Electronics Conference (COBEP/SPEC). IEEE, 2019.

[21] Sola, Jorge, and Joaquin Sevilla. "Importance of input data normalization for the application of neural networks to complex industrial problems." IEEE Transactions on nuclear science 44.3 (1997): 1464-1468.

[22] Zhao, Zhizhong, et al. "Application and comparison of BP neural network algorithm in MATLAB." 2010 International Conference on Measuring Technology and Mechatronics Automation. Vol. 1. IEEE, 2010.

[23] Du, Bolun, et al. "Intelligent classification of silicon photovoltaic cell defects based on eddy current thermography and convolution neural network." IEEE Transactions on Industrial Informatics 16.10 (2019): 6242-6251.

[24] Li, Xiaoxia, et al. "Deep learning based module defect analysis for large-scale photovoltaic farms." IEEE Transactions on Energy Conversion 34.1 (2018): 520-529.